Proceedings of the 11th Brazilian Congress of Thermal Sciences and Engineering – ENCIT 2006
Braz. Soc. of Mechanical Sciences and Engineering – ABCM, Curitiba, Brazil, Dec. 5-8, 2006

Paper CIT06-0103

Turbulence challenges: flow separation and roughness effects

Atila P. Silva Freire
PEM/COPPE/UFRJ, C.P. 68503, 21945-970 – Rio de Janeiro, Brazil
atila@mecanica.coppe.ufrj.br

Abstract. *The present work strives on showing how two very important and difficult problems in engineering, flow separation and flow over rough surfaces, can be given an elegant treatment. After some detailed consideration on the fundamentals of each problem, the advanced theories are tested against respectively: i) flows over steep hills and ii) flows in micro-channels. Much emphasis is placed here on the description of the near wall turbulence.*

Keywords: *Turbulence, separation, roughness, hill, micro-channel.*

1. Introduction

Fluid dynamics is a profoundly difficult subject with a host of engineering applications. The trouble is that despite the many comprehensive advances that were achieved over the past century, some key and fundamental problems still remain unsolved. Complex engineering projects are then very often obliged to compromise, seeking solutions yielded by *ad hoc* procedures that lack a rigorous treatment.

Turbulence is a most notable problem in fluid dynamics. The presence of a highly irregular variation of the velocity field with time and space makes the flow description extremely complicated. Turbulent flow is an infinite dimension nonlinear system that has to be defined accordingly to some initial conditions. In real flows, the specification of the exact initial conditions from which the equations of motion can be integrated is, however, physically meaningless. Indeed, the exact microscopic description of a given flow would necessarily require the specification of both the position and the velocity of every lump of fluid. This is clearly an impossible undertaking.

If, on the other hand, we recover the notion that in a turbulent flow the fluid particles move in an extremely complex and irregular way, we may consider that over some sufficiently long time interval the effects of the initial conditions on the flow are smoothed out and disappear. Hence, this suggests that turbulent flows may be prone to a statistical representation. Unfortunately, no full theory of turbulence has been developed so far.

The purpose of this work is to show how two very important – but yet very difficult – problems facing turbulence modelers can be tackled: the prediction of separation and of roughness effects on flow properties. These are problems that have been around for a long time now but that still deserve a definitive and rigorous treatment.

In fact, these two problems must be very highly ranked in any list that considers the major unsolved problems of fluid mechanics. Thus, it may appear to the reader that we are faced with an impossible endeavor: the elucidation of problems that have been for years the central concern of researches but that have been left open. Actually, we will show how different thinking schools were developed to provide some useful results on both subjects. This will be made separately. After a section on fundamentals, where a common ground of discussion is established, two other sections will follow where the problem of a separating flow and the problem of flows over a rough surface are discussed.

2. Fundamentals

The equations of motion for a flow of an incompressible fluid are the Navier-Stokes equations:

$$\partial_t u_i + u_j \, \partial_j u_i = -\partial p + \nu \partial^2 u_i, \tag{1}$$

$$\partial_i u_i = 0 \tag{2}$$

where the pressure term incorporates the density and ν denotes the kinematic viscosity.

The above equations must be supplemented by initial and boundary conditions. They describe the motion of many common fluids, including air, water, alcohol, glycerine and most gases. Other more complicated fluids

require different constitutive relationships between the rate of strain and the induced stress. The present work will only deal with flows that are governed by Eqs. 1 to 2.

As it turns out, turbulence is a very irregular phenomenon – in time and space – what makes its detailed description a very difficult affair. However, we have already mentioned in the introduction that a probabilistic approach to turbulence might be a good choice. This would be very in hand since average values of important flow properties such as velocity, pressure, temperature, *et cetera*, would become available. Therefore, we may say that average quantities taken in terms of time, space or ensembles can be defined accordingly to certain characteristic scales of the flow.

Now consider that the Navier-Stokes equations must hold for any instant but also on the average; it results that a decomposition of the flow variables into mean and fluctuating parts yields:

$$\partial_t \overline{u_i} + \overline{u_j}\,\partial_j \overline{u_i} = -\partial \overline{p} + \nu \partial^2 \overline{u_i} - \partial_j \overline{u_i' u_j'}, \tag{3}$$

$$\partial_i \overline{u_i} = 0 \tag{4}$$

where the overbars are used to denote a mean quantity, e.g. in time, and the dashes a fluctuating quantity.

The two equations above are referred to in literature as the Reynolds Averaged Navier-Stokes equations (RANS). They introduce an additional term – the Reynolds stresses ($-\partial_j \overline{u_i' u_j'}$) – which represents the transport of momentum due to turbulent fluctuations.

The above formal procedure naturally isolates the effects of the fluctuations on the mean flow. However, Eq. 3 contains nine unknown quantities that have to be defined through complementary differential or algebraic relationships. This defines what is known as the *closure problem* of turbulence, a very often frustrating prospect.

Before we move forward, we point out to the reader that the simplest possible way of modelling the turbulent terms is to consider that the turbulent stresses act like the viscous stresses so that we may write

$$-\overline{u_i' u_j'} = \nu_t \left(\partial_j \overline{u_i} + \partial_i \overline{u_j}\right) \tag{5}$$

where ν_t denotes the eddy viscosity.

Then by analyzing the random motion of lumps of fluid in a turbulent shear flow (Tennekes and Lumley (1972)), we may consider ν_t to depend on characteristic length and velocity scales. Near to a rigid wall,

$$\nu_t = u_c l_c, \quad u_c = l \left| d\overline{u_1}/dx_2 \right|, \quad l = \varkappa x_2, \, \varkappa = 0.4 \tag{6}$$

In the next sections we will show in full extent how such simple reasonings can result in such powerful results.

3. Flow near a separation point

Boundary layer separation from a rigid body is one of the most challenging problems in fluid dynamics. Classical books including the texts of Goldstein (1938), Landau and Lifshitz (1959) and Batchelor (1967) do not hesitate in saying that "separation is the aspect of laminar flow at high Reynolds number that presents the greatest theoretical difficulty" (Batchelor (1967)). If that is really the case, one may then just wonder the type of difficulties that turbulent separation should hold for us.

Thus, before we consider turbulent separation, let us first establish some results from laminar theory.

3.1. Laminar separation

Goldstein (1948) showed that a crucial result in the theory of separated flow are the compatibility conditions for the boundary layer equations (BLE) at a point of zero wall shear stress. The complicated conditions that arise for the investigation of singularities in separated flows show that, whenever they occur, the boundary layer equations cease to be valid at and near separation, on both its downstream and upstream sides. In fact, a classical result of boundary layer theory is that u_1 $(= u)$ is much large as compared to u_2 $(= w)$. The implication is that fluid particles move predominantly along the wall of the body, and only very slightly away from it. Thus, separation cannot occur but for the presence of singularities in the BLE.

We also know from the boundary layer theory that w/u is of the order of $1/\sqrt{R}$. Hence, if a singularity is reached by the flow in which w and u are to become of the same order this implies an increase of w by a factor of $\sqrt{R}$. In the limit of large Reynolds numbers, we have

$$w(x_s, z) = \infty, \tag{7}$$

where x_s denotes the position of flow separation and z the distance from the wall.

The above reasonings with $\partial w/\partial z = \infty$, together with the continuity equation imply that

$$\text{order}(\partial u/\partial x) = \text{order}(\partial w/\partial z) = \infty, \tag{8}$$

which furnishes immediately $(\partial x/\partial u) = 0$.

Near a point of separation, $x_s - x$ can be expanded in powers of $u - u_s$ provided we take notice that the first-order term in the expansion vanishes identically ($(\partial x/\partial u)_{u=u_s} = 0$). The result is

$$(x_s - x) = A(z)(u - u_s(z))^2, \quad \text{or} \quad u = u_s(z) + B(z)\sqrt{(x_s - x)}, \quad B = 1/\sqrt{A}. \tag{9}$$

Summoning again the equation of continuity,

$$\frac{\partial w}{\partial z} = -\frac{\partial u}{\partial x} = \frac{B(z)}{2\sqrt{x_s - x}} \tag{10}$$

which upon a first integration gives

$$w = \frac{C(z)}{\sqrt{x_s - x}}, \qquad C(y) = (1/2)\int B(z)dz. \tag{11}$$

The above results when applied to the boundary layer equations,

$$\underbrace{u\frac{\partial u}{\partial x} + w\frac{\partial u}{\partial z}}_{infinity} = \underbrace{-\frac{\partial p}{\partial x} + \nu\frac{\partial^2 u}{\partial z^2}}_{limited\ values}, \tag{12}$$

show that both terms on the left-hand side become infinite whereas those on the right-hand side remain limited. Thus, on a first approximation, the flow near to a separation point is a wake-like flow dominated by inertial effects and governed by the equation

$$u\frac{\partial u}{\partial x} + w\frac{\partial u}{\partial z} = 0. \tag{13}$$

The character of the singularity is then such that the transversal wall velocity increases as $(x_s - x)^{-1/2}$ as the separation point is approached.

Substituting $\partial u/\partial x$ = -$\partial w/\partial z$, we may write

$$u\frac{\partial w}{\partial z} - w\frac{\partial u}{\partial z} = u^2\frac{\partial}{\partial z}\left(\frac{w}{u}\right) = 0, \tag{14}$$

that is, we conclude that w/u is independent of z.

The above picture of the problem is given by Landau and Lifschitz (1959). Goldstein (1948) had already constructed a very rigorous theory to show that immediately ahead of separation the boundary layer equations assume a two-layered structure with an inner wall region that decreases according to $z \approx (-x)^{1/4}$. Goldstein also demonstrated that it is impossible to continue the boundary layer solution through the point $x = 0$.

The way out to the troubles considered above is to abandon the hypothesis of regularity of the pressure distribution at the boundary layer separation point. Thus, for flows near to a separation point there is an interaction of the boundary layer flow with the external potential flow such that the pressure gradient leading to separation is always self-induced.

To describe the flow structure in regions of strong interaction, the Prandtl-boundary layer theory has to be specialized and multi-layered structures considered. A typical feature is that the viscous layer is divided into two further layers. One may then speak of triple-deck theory (TD). Stewartson (1969) showed that if massive separation occurs, then TD *cannot* remove Goldstein's singularity. Indeed, the positive pressure gradient imposed on the boundary layer is the important obstacle.

3.2. Turbulent separation

Turbulent separation is a specially difficult problem. In addition to all the conceptual difficulties we saw at the previous section, turbulent flows also require the choice of a representative turbulence model. The possibilities are many. However, in the present work we restrain ourselves to the analysis of simple algebraic models. The type of model that was introduced by Eqs. 5 and 6. The criticism here might be strong since one may argue that mixing-length and eddy viscosity models are physically meaningless in the reverse flow region and have small values in the outer region of the separated flow. In the vicinity of the separation, just ahead of the point of separation itself, however, mixing-length can be taken as a good approximation (Simpson et al. (1981)).

The structure of a turbulent boundary layer far away from a singularity point was studied by Yajnik (1970) through the matched asymptotic method. Working with an underdetermined system of equations, i.e. without any closure consideration, Yajnik showed that the boundary layer can be divided into different layers whose properties can be described through two reference length scales. The resulting expansions present a non-uniformity at the point of zero skin-friction, so that they are not applicable to separating flows. This work was soon followed by contributions by Bush and Fendell (1972) and Mellor (1972) that helped to consolidate a consistent large Reynolds number asymptotic theory for turbulent boundary layers. Of course, as it turns out, all theories present a non-uniform behaviour near a separation point.

To describe the flow in the neighborhood of a point of separation, Sychev and Sychev (1980) employed a multi-structured analysis in which the boundary layer is divided into ten different layers. Without resorting to any closure model, the work uses asymptotic arguments to construct local solutions that can be matched to provide a composite solution. The approaching flow is split into four regions, whereas the interaction region is split into six. The principal findings are that i) the longitudinal mean velocity varies in proportion to $(x_s - x)^{1/4}$, ii) the boundary layer thickness increases as $\ln(x_s - x)$, and iii) the wall shear stress decreases in proportional to $(x_s - x)^{1/2}$. A problem with the theory of Sychev and Sychev is its inability to provide an explanation of how the logarithmic near wall behavior ceases to exist as separation is reached.

The asymptotic structure of a separating turbulent boundary layer was addressed by Melnik (1989) through a complete different route. His new asymptotic theory is based on formal expansions in terms of two parameters: Reynolds number and a constant appearing in the eddy-viscosity model, α. The inner layer solution shows that $\Delta x = \mathrm{O}(\alpha^{1/2})$ is the appropriate length scale near separation. The appearance of a slip velocity with a square root singularity at separation is justified as the main reason for the difference in structure between the laminar and turbulent flow limit solutions.

More recently, other different arguments were used to investigate the asymptotic structure of a separating boundary layer. The single limit concept of Kaplun (1967) was used by Cruz and Silva Freire (1998, 2002) to show how the canonical two-layered structure of the turbulent boundary layer can be described in terms of principal and intermediate equations. The two relevant reference lengths derived by Cruz and Silva Freire (1998) are u_τ^2/U_∞^2 and ν/u_τ. An important point to ponder here is that as a separation point is approached u_τ^2/U_∞^2 decreases whereas ν/u_τ increases. Thus, at a certain distance from the separation point, order(u_τ^2/U_∞^2) = order(ν/u_τ) and the two principal equations merge giving origin to a new structure where the log-solution ceases to exist and the flow solution is given by a combination of a wake-like solution to a viscous solution. In particular, at the very separation point, the flow has a wake solution. Concerning the reference velocity scales, u_R, the authors have shown that scaling analysis can be used to yield

$$u_R^3 - \frac{\tau_w}{\rho} u_R - \frac{\nu}{\rho}\frac{\partial p}{\partial z} = 0. \tag{15}$$

The highest real root from the above algebraic equations gives u_R. Please note that in the limiting cases $\partial p/\partial z \to 0$ and $\tau_w \to 0$, the reference scales reduce respectively to

$$u_R = \sqrt{\frac{\tau_w}{\rho}} = u_\tau, \qquad u_R = \left(\frac{\nu}{\rho}\frac{\partial p}{\partial z}\right)^{1/3}, \tag{16}$$

so that the classical reference scales commonly referred to in literature are recovered. This will be reviewed shortly next.

3.3. Near wall approximations for separating flows

The previous text must have given the reader a clear picture of the difficulties involved in describing the flow near to a wall and to a separation point. Because turbulent flows are rich in scales and the reference near wall scales are very small, typically of the order of ν/u_τ, any numerical simulation of a flow field will have to resort to very fine meshes. This, of course, imposes a heavy penalty on computations that have to be performed over large flow regions. One popular way to overcome this problem is to avoid the near wall region with the specification of an approximate solution at some distance from the wall. The solution procedure then follows the principles enunciated above. Through an asymptotic analysis of the problem, local equations are deducted to yield local solutions. At the near wall region, domains can then be identified where viscous and turbulent effects are the dominant effects. Provided the flow is far from a separation point, local solutions for the turbulence dominated region will result in a logarithmic velocity profile. This can then be used as a wall boundary conditions to the external flow solution. Just for the records, the log-solution in boundary layer theory is normally referred to in literature as the "law of the wall".

In the present section, some different notions of the law of the wall be reviewed. Despite the critics of many researchers, the use of wall functions to by-pass the difficulties involved with the modeling of low Reynolds

number turbulence is still an attractive means to solve problems in a simple way. We must warn the reader that some of the derivations are quite evolving, a recurring feature that has really prevented us from going into too much detail. Still, to assure legibility of the paper, the most relevant equations will be presented here in full. For a complete account of the formulations, the reader is referred to the original references.

3.3.1. The logarithmic law of wall formulation for a smooth wall

For turbulent attached flows over a smooth wall, Prandtl (1925) considered the existence of a region adjacent to the wall in which the total shear stress is nearly constant. Bearing in mind that viscosity must play a role in finding local solutions, a simple scaling analysis furnishes u_τ and ν/u_τ as the two relevant scaling parameters.

The analysis may follow either from dimensional arguments or by mixing-length theory. Here, the second route is taken. Then, for the turbulent part of the wall region we may write

$$\frac{\partial \tau_t^+}{\partial z^+} = \frac{\partial}{\partial z^+}(-\overline{u'^+ w'^+}) = \frac{\partial}{\partial z^+}\left(\varkappa^2 z^{+^2}\left(\frac{\partial u^+}{\partial z^+}\right)^2\right) \tag{17}$$

where the notation is standard. The dash denotes quantity fluctuation, $u^+ = u/u_\tau$, $\tau_t^+ = \tau_t/(\rho u_\tau^2)$, $\tau_t = -\rho\overline{u'w'}$, $\overline{u'^+ w'^+} = \overline{u'w'}/u_\tau^2$ and $z^+ = z/(\nu/u_\tau)$.

Upon two successive integrations, we have

$$u^+ = \varkappa^{-1} \ln z^+ + A, \tag{18}$$

the classical law of the wall for a smooth surface ($\varkappa = 0.4$, $A = 5.0$) and zero-pressure gradient flows.

Equation (18) presents clear difficulties as $u_\tau \to 0$.

3.3.2. Stratford's equation

The action of an arbitrary pressure rise in the inner layer will distort the velocity profile until it is balanced by the gradient of shear stress. At the wall, inertia forces are zero so that this balance is expressed by

$$\frac{\partial p}{\partial x} = \frac{\partial \tau}{\partial z}. \tag{19}$$

A first integration of the above equation yields

$$\tau = z\frac{\partial p}{\partial x}, \quad (\tau_w = 0, z \text{ small}) \tag{20}$$

where we have used the fact that at separation the wall shear stress, τ_w, is zero.

Using the mixing-length theory to model τ, together with the condition u=0 at z =0, Eq. (20) integrates to

$$u = \left(\frac{4}{\rho\varkappa^2}\frac{\partial p}{\partial x}\right)^{1/2} z^{1/2}, \quad (\tau_w = 0, z \text{ small}) \tag{21}$$

that is,

$$u^+ = \frac{2}{\varkappa} z^{+1/2} \tag{22}$$

the so-called Stratford equation, where

$$u^+ = u/u_R,\ z^+ = z/(\nu/u_R), \qquad \text{with} \qquad u_R = \left(\frac{\nu}{\rho}\frac{\partial p}{\partial x}\right)^{1/3}. \tag{23}$$

3.3.3. The law of the wall formulation of Mellor (1966)

The effect of pressure gradients on the behaviour of turbulent boundary layers without restriction to equilibrium was investigated by Mellor (1966) through dimensional arguments. When a large external pressure gradient is applied to a boundary layer, no portion of the defect profile overlaps the logarithmic law. In fact, as previously suggested by Coles (1956) and by Stratford (1959), very near a separation point the logarithmic part of velocity profile ceases to exist. However, if Millikan's (1939) arguments are recast and a new pressure gradient parameter is included in the analysis, an equation can be derived which satisfies the required limiting form as a separation point is approached.

Making the approximation that in the viscous sublayer the stress terms should be balanced only by the pressure term in the motion equations, Mellor (1966) found

$$u^+ = z^+ + \frac{1}{2}p^+ z^{+2} \tag{24}$$

for the inner region of the boundary layer, whereas for the outer layer he wrote

$$u^+ = \xi_{p^+} + \frac{2}{\varkappa}\Big(\sqrt{1+p^+z^+}-1\Big)+\frac{1}{\varkappa}\ln\Big(\frac{4z^+}{2+p^+z^+ +2\sqrt{1+p^+z^+}}\Big) \tag{25}$$

where $z^+ = zu_{p\nu}/\nu$, $u^+ = u/u_{p\nu}$, $u_{p\nu} = [(\nu/\rho)(dp/dx)]^{1/3}$ and $p^+ = [(\nu/\rho)(dp/dx)]/u_\tau^3$. Depending on whether parameter p^+ is small or large, Eq. (25) will follow different asymptotic behaviours in the limiting cases $p^+ \to 0$ or ∞, tending respectively to the classical logarithmic law or to Stratford's equation. Regarding, $u_{p\nu}$, depending on the limiting values of p^+, $u_{p\nu} \to u_\tau$ (small values of p^+) or $u_{p\nu} \to u_{p\nu}$=$[(\nu/\rho)(dp/dx)]^{1/3}$ (large values of p^+). Function ξ_{p^+} is a known parameter having been determined numerically for a range of p^+'s (Table 1).

Eqs. (24) and (25) were specified for the viscous and logarithmic regions respectively. For numerical purposes, these regions were considered to intersect at $z^+ = 11.64$, which was considered to be the point of mathematical intersection of the viscous and logarithmic regions for the classical law of the wall. Regarding the law of the wall formulations which take into account the effects of adverse pressure gradients, the mathematical intersection of the inner and logarithmic functions depends on the value of the dimensionless pressure p^+.

p^+	-0.01	0.00	0.02	0.05	0.1	0.2	0.5	1	2	10
ξ_{p^+}	4.92	4.90	4.94	5.06	5.26	5.63	6.44	7.34	8.49	12.13

Table 1: Integration function (Mellor (1966)), p^+.

3.3.4. The law of the wall formulation of Nakayama and Koyama (1984)

Nakayama and Koyama (1984) obtained a law of the wall for boundary layers subjected to adverse pressure gradients by conducting a one-dimensional analysis on the turbulent kinetic energy equation with assumptions of local similarity. Considering the two possible limiting cases of a constant stress layer and of a zero wall stress layer, the authors propose a turbulent kinetic energy equation that upon integration yields,

$$u^+ = \frac{1}{\varkappa^+}\Big[3(\zeta-\zeta_s)+\ln\Big(\frac{\zeta_s+1}{\zeta_s-1}\frac{\zeta-1}{\zeta+1}\Big)\Big] \tag{26}$$

where

$$\zeta = \Big(\frac{1+2\tau^+}{3}\Big)^{1/2} \tag{27}$$

The above formulation introduces a Von Kármán modified constant, $\varkappa^+$, and the slip value, ζ_s. For a boundary layer subjected to an adverse pressure gradient,

$$\tau^+ = 1+p^+z^+, p^+ = \nu\rho^{1/2}(d\tau/dz)_w/\tau_w^{3/2}, z^+ = (\tau_w/\rho)^{1/2}z/\nu \tag{28}$$

The Von Kármán modified constant was estimated to be

$$\varkappa^+(p^+) = \frac{0.419+0.539p^+}{1+p^+} \tag{29}$$

The slip value ζ_s was determined from the condition that in the limiting case $p^+ \to 0$ the above formulation reduces to the classical law of the wall, Eq. (18). It follows that

$$\zeta_s(p^+) = (1+(2/3)e^{-\varkappa A}p^+)^{1/2} \approx (1+0.074p^+)^{1/2} \tag{30}$$

Nakayama and Koyama (1984) considered their analysis general in the sense that velocity was related to the local shear stress instead of to the distance from the wall. Additionally, the analysis does not have to be restricted to a linear velocity-stress relation but can be applied for any monotonically increasing shear stress layer.

3.3.5. The law of the wall formulation of Cruz and Silva Freire (1998, 2002)

Introducing a new scaling procedure, Cruz and Silva Freire (2002) proposed the law of the wall for a separating flow to be written as

$$u = \frac{\tau_w}{|\tau_w|}\frac{2}{\varkappa}\sqrt{\frac{\tau_w}{\rho} + \frac{1}{\rho}\frac{dP_w}{dx}z} + \frac{\tau_w}{|\tau_w|}\frac{u_\tau}{\varkappa}\ln\left(\frac{z}{L_c}\right), \tag{31}$$

where

$$L_c = \frac{\sqrt{\left(\frac{\tau_w}{\rho}\right)^2 + 2\frac{\nu}{\rho}\frac{dP_w}{dx}u_R} - \frac{\tau_w}{\rho}}{\frac{1}{\rho}\frac{dP_w}{dx}}, \tag{32}$$

$\varkappa = 0.4$, u_τ is the friction velocity, and u_R ($= \sqrt{\tau_p/\rho}$, $\tau_p =$ total shear stress) is a reference velocity.

The total shear stress, τ_p, can be evaluated from

$$\tau_p = C_\mu^{1/2}\rho\kappa_p + \mu\left|\frac{\partial u}{\partial z}\right|_p \tag{33}$$

where the subscript p denotes the first grid point, C_μ (=0.09) is a constant and κ the turbulent kinetic energy.

The reference velocity u_R can then be directly determined from

$$u_R = \sqrt{\frac{\tau_p}{\rho}}. \tag{34}$$

Equation (33) was obtained from a momentum balance in the near wall region; it is similar to a relation usually employed by other authors to relate the wall shear stress to the turbulent kinetic energy in a κ-ϵ formulation (see, e.g., Launder and Spalding (1974), the only difference here is the inclusion of the viscous term to improve calculations when $z/L_c \leq 30$.

To find a first estimate for the wall shear stress, τ_{wo}, Eqs. (18) and (33) can be combined to give

$$\tau_{wo} = \frac{u_p C_\mu^{1/4}{\tau_p}^{1/2}\rho^{1/2}\varkappa}{\ln\left(E\, z\, \frac{(\tau_p/\rho)^{1/2}}{\nu}\right)}. \tag{35}$$

with $E = e^{\varkappa A}$.

The pressure gradient at the wall can be obtained through Eqs. (33) and (35),

$$\frac{dP_w}{dx} = \frac{\tau_p - \tau_{wo}}{z_p}. \tag{36}$$

This equation was obtained directly from the inner layer approximated equations; it represents the balance of forces in that layer.

Next, the characteristic length can be calculated from

$$L_c = \frac{\sqrt{\left(\frac{\tau_{wo}}{\rho}\right)^2 + 2\frac{\nu}{\rho}\frac{dP_w}{dx}u_R} - \frac{\tau_{wo}}{\rho}}{\frac{1}{\rho}\frac{dP_w}{dx}}. \tag{37}$$

Finally, the wall shear stress is calculated from Eq. (31) according to

$$\tau_w = \frac{u_p{\tau_p}^{1/2}\rho^{1/2}\varkappa}{2\sqrt{\left|\frac{\tau_p}{\tau_{wo}}\right|} + \ln\left(\frac{z_p}{L_c}\right)}. \tag{38}$$

Using some production-dissipation equilibrium assumptions and Eq. (31) the kinetic energy dissipation and the production terms can be written respectively as follows:

$$\text{Dissipation} = C_\mu{}^{\frac{1}{2}}\kappa_p\left(\frac{(\tau_p/\rho)^{1/2}}{\varkappa z} + \frac{\frac{1}{\rho}\frac{dP_w}{dx}}{\varkappa(\tau_p/\rho)^{1/2}}\right), \tag{39}$$

$$\text{Production} = \frac{C_\mu{}^{\frac{1}{2}}\kappa_p\rho}{z}\left(\frac{2(\tau_p/\rho)^{\frac{1}{2}}}{\varkappa} + \frac{|\,(\tau_{wo}/\rho)\,|^{\frac{1}{2}}}{\varkappa}\ln\left(\frac{z}{L_c}\right)\right). \tag{40}$$

Table 2: Main characteristics of the laser-Doppler system

Wavelength	514.5 nm
Half-angle between beams	3.415^o
Fringe spacing	4.3183 μm
Frequency shift	0.60 MHz
Dimensions of the measurement volume	
Major axis	1.53 mm
Minor axis	162.0 μm

Equation (31) is a generalization of the classical law of the wall and replaces the three expressions advanced in Cruz and Silva Freire (1998), Eqs. (25, 26, 27). Eq. (32) is an expression for the near wall region characteristic length, which is assumed to be valid in the attached and in the reverse flow regions.

Far away from the separation point, where the wall shear stress is positive and $z(dP_w/dx) << \tau_w$, Eq. (31) reduces to the classical law of the wall, Eq. (18),

$$u = \frac{2}{\varkappa} u_\tau + \frac{u_\tau}{\varkappa} \ln(\frac{z}{L_c}), \quad L_c = \nu/u_\tau. \tag{41}$$

Near to the separation point where $\tau_w = 0$, Eq. (31) leads to

$$u = \frac{2}{\varkappa} \sqrt{\frac{z}{\rho} \frac{dP_w}{dx}}, \tag{42}$$

an equation similar to Stratford's equation, Eq. (21) (see Stratford (1959)).

In the reverse flow region where the wall shear stress is negative and $z(dP_w/dx) << \tau_w$, equation (31) reads

$$u = -\frac{2}{\varkappa} u_\tau - \frac{u_\tau}{\varkappa} \ln(\frac{z}{L_c}), \quad L_c = 2\left|\frac{\tau_w}{dP_w/dx}\right|. \tag{43}$$

The generalization provided by Eq.(31) implies that the friction velocity, u_τ, used in the definition of L_c had to be replaced by the reference velocity u_R. Please, note that the characteristic length in the reverse flow region is different from the classical characteristic length given the classical law of the wall. Equation (43) is in agreement with Simpson et al. (1981), who suggested that a characteristic length for the backflow region should be directly proportional to the absolute value of the wall shear stress.

3.3.6. Theory validation

The theories presented above will now be tested against some experimental data. Of course, two parameters are of major importance for a good assessment of the proposed expressions: mean velocity and wall shear stress profiles. Also an important issue is the geometry to be chosen. Flows over steep hills are a particular difficult test for theories.

Here, we will use the data of Loureiro et al. (2006) of turbulent flow over a steep, smooth hill to compare the theories. Therefore, for further details on the flow conditions the reader is referred to the original paper. In fact, all results presented in this section were taken from Loureiro et al. (2006).

The experiments were performed in the open–channel of the Hydraulics Laboratory of the Civil Engineering Department, University of Oporto, Portugal. The water channel is a 17 m long channel with a cross section of 40 cm width per 60 cm height. The recirculation system consists two underground tanks, a top stabilization tank, and four pumps with a maximum total capacity of 150 l/s. The working section has glass side walls, 3 m in length, and is situated 7.3 m downstream of the channel entrance. The model hill was located 8 m from the channel entrance.

A one component, fiber optic, Dantec laser-Doppler anemometry system was used in the forward scatter mode to measure the mean and the fluctuating velocity fields. The characteristics of the measuring system are given in a Table 2. This system was used to measure both the longitudinal and the vertical velocity components. This was easily made by simply turning the probe 45 deg. around its axis, so that, on both conditions, the fringe distribution was perpendicular to the measured velocity component. Typical uncertainties associated to the mean and fluctuating velocity data, $\overline{U}$, $\overline{W}$, σ_u, σ_w and σ_{uw} were estimated as ± 2.5 %, ± 10 %, ± 6.5 %, ± 6.5% and ± 12 %, respectively.

The model hill used in the present work was two-dimensional and aerodynamically smooth and was defined through equation

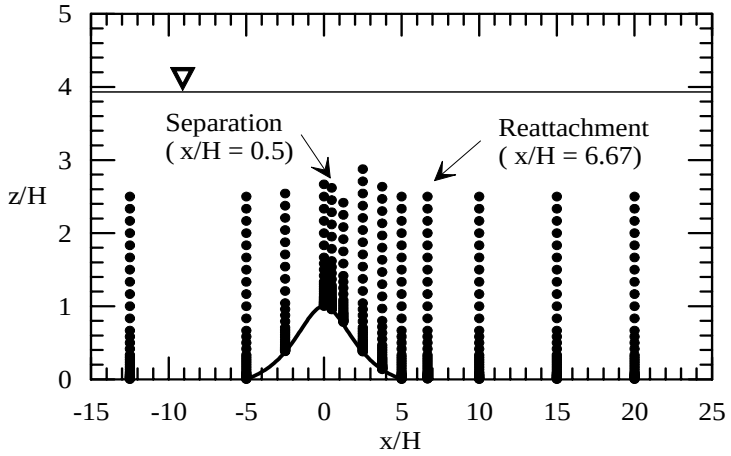

Figure 1: Position of measuring stations and co-ordinate system.

$$z_H(x) = H_1[1 + (x/L_H)^2]^{-1} - H_2 \tag{44}$$

where H (=H_1-H_2)(= 60 mm) is the hill height and L_H (= 150 mm) is the characteristic length of the hill representing the distance from the crest to the half-height point. Co-ordinates, x and z represent the horizontal and vertical axes, respectively.

Measurements were made on the channel centerline at the thirteen stations illustrated in Fig. 1.

The wall shear stress was evaluated from linear fits to the viscous region velocity profiles. In the first 3 mm away from the wall, eight points were considered for the flow characterization and the determination of τ_w.

The numerical simulations were carried out with the code Turbo-2D (Fontoura Rodrigues (1990)), which is a two-dimensional code based on the finite elements method. The application of standard Garlekin discretization to problems that are dominated by convection, frequently leads to non-physical oscillations and convergence difficulties. To alleviate this tendency, code Turbo-2D resorts to the balance dissipation method proposed by Hughes and Brooks (1979) and Kelly et al. (1980) and implemented by Brun (1988). The structure of code Turbo-2D was based on the work of Brison et al. (1985), which uses finite elements of type P1-isoP2 for space discretization and semi-implicit time discretization.

The governing equations for Turbo-2D are the Reynolds averaged equations for an incompressible flow complemented by the eddy viscosity formulation and the standard κ-ϵ model.

Regarding the experimental conditions, the inflow values of the mean velocity, of the turbulence kinetic energy and of the dissipation rate were taken directly from the experimental data. In the region adjacent to the surface, wall functions were used as explained next. At the top, a free surface condition was used. For the outflow, symmetry (zero normal gradient) conditions were applied.

Typical values of computational times for the various law of the wall formulations are shown in Table (3).

Table 3: Correspondent flow time required to achieve numerical convergence for each law of the wall formulation simulated.

Formulation	LogLaw	M (1966)	NK (1984)	CSF (1998)
Time (seconds)	100	2000	2500	2500

The computations were performed with a very fine mesh with 13888 nodes (P1-isoP2). Here we should point out to the reader a mesh with 13888 nodes is considered to be extremely fine for finite elements standards. The computational grid is shown in Fig. 2.

The general flow pattern is shown in Fig. 3. Mean velocity profiles obtained by the different law of the wall formulations are presented in Fig. 4 for the region of separate flow.

The location of flow detachment was best predicted by the model of Nakayama and Koyama (1974). Unfortunately, this same model over predicted the position of flow re-attachment by 34%, as illustrated in Fig. 3d. The formulation of Cruz and Silva Freire (1998) over predicts detachment and under predicts reattachment, resulting in a separated region 13.5% shorter than the experimentally determined length (Fig. 3b). The results obtained through Mellor's formulation over predicted both the detachment and the reattachment points, as shown in Fig. 3c. This yielded a separation region with length $x/H = 6.00$, a value very close to the experimental value, x/H

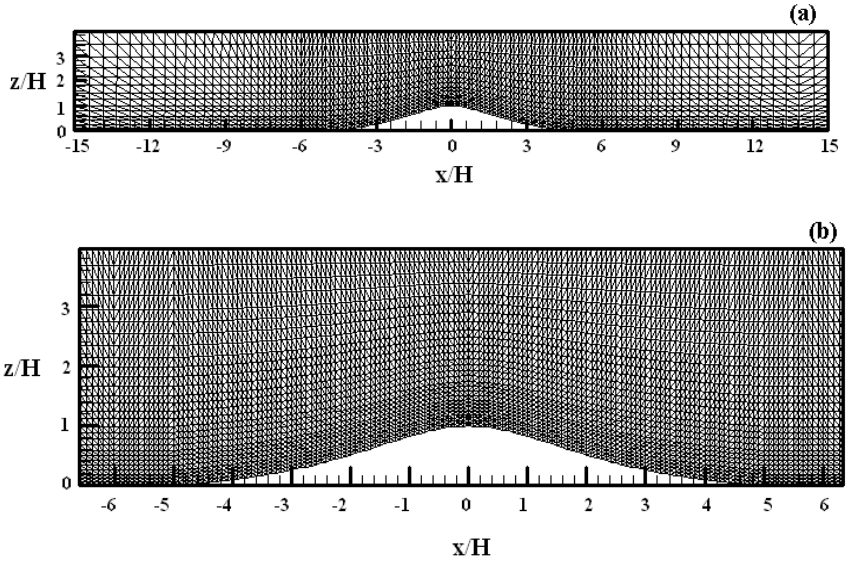

Figure 2: Typical mesh distribution around hill for pressure and velocity fields evaluation. (a) P1 mesh with 1875 nodes and 3472 elements. (b) Iso/P2 mesh with 7221 nodes and 13888 elements.

= 6.17. Under the present mesh conditions, the classical law of the wall was shown to be incapable of promoting flow separation. For the other formulations, however, the differences were marked. Table (4) summarizes the main findings.

Table 4: Length of separation bubbles according to different formulations.

Formulation	Detachment (x/H)	Reattachment (x/H)	Length (x/H)
LogLaw	not predicted	not predicted	not predicted
M (1966)	0.90	7.00	6.00
NK (1984)	0.60	8.90	8.30
CSF (1998)	0.80	6.10	5.30
Experiment	0.50	6.67	6.17

The different mean velocity predictions for the different law of the wall formulations are marked. The results provided by the classical law of the wall fail completely in predicting the separation region. Overall, the predictions obtained through the formulations of Mellor (1966) and of Nakayama and Koyama (1974) give a slower recovery of the mean velocity to the downstream undisturbed levels. Thus for most of the far wall separation region, velocity is under predicted by the models of Mellor (1966) and of Nakayama and Koyama (1974). The near wall formulation of Cruz and Silva Freire (1998) do provide the best results. However, the very strong reverse flow region shown very close to the wall at stations $x/H = 2.5$ and 3.75 was not well predicted in any sense by all three models.

The wall shear stress distribution is shown in Fig. 5. The curves illustrate the findings provided by the four different numerical simulations. Downstream of the hill, all simulations performed well. On the hill top, the inability of the models to resolve the near wall layer resulted in a large overestimation of τ_τ. This is a direct consequence of the largely overestimated near wall velocity gradients. Clearly, the bad predictions in the reversed flow region are due to the simulations that, in fact, could not predict the existence of such region. The models that were capable of resolving the inner flow regions with some accuracy were the ones that furnished the best wall shear stress predictions.

4. Flow over roughness

The description of turbulent flow over a rough surface has been a major concern to researchers over the past eighty years. Because natural surfaces are characterized by a great number of geometrical parameters, their detailed mathematical modeling is a virtually impossible exercise. The following statement by Schlichting is typical in texts: "The desire to explore the laws of friction of rough pipes in a systematic way is frustated by

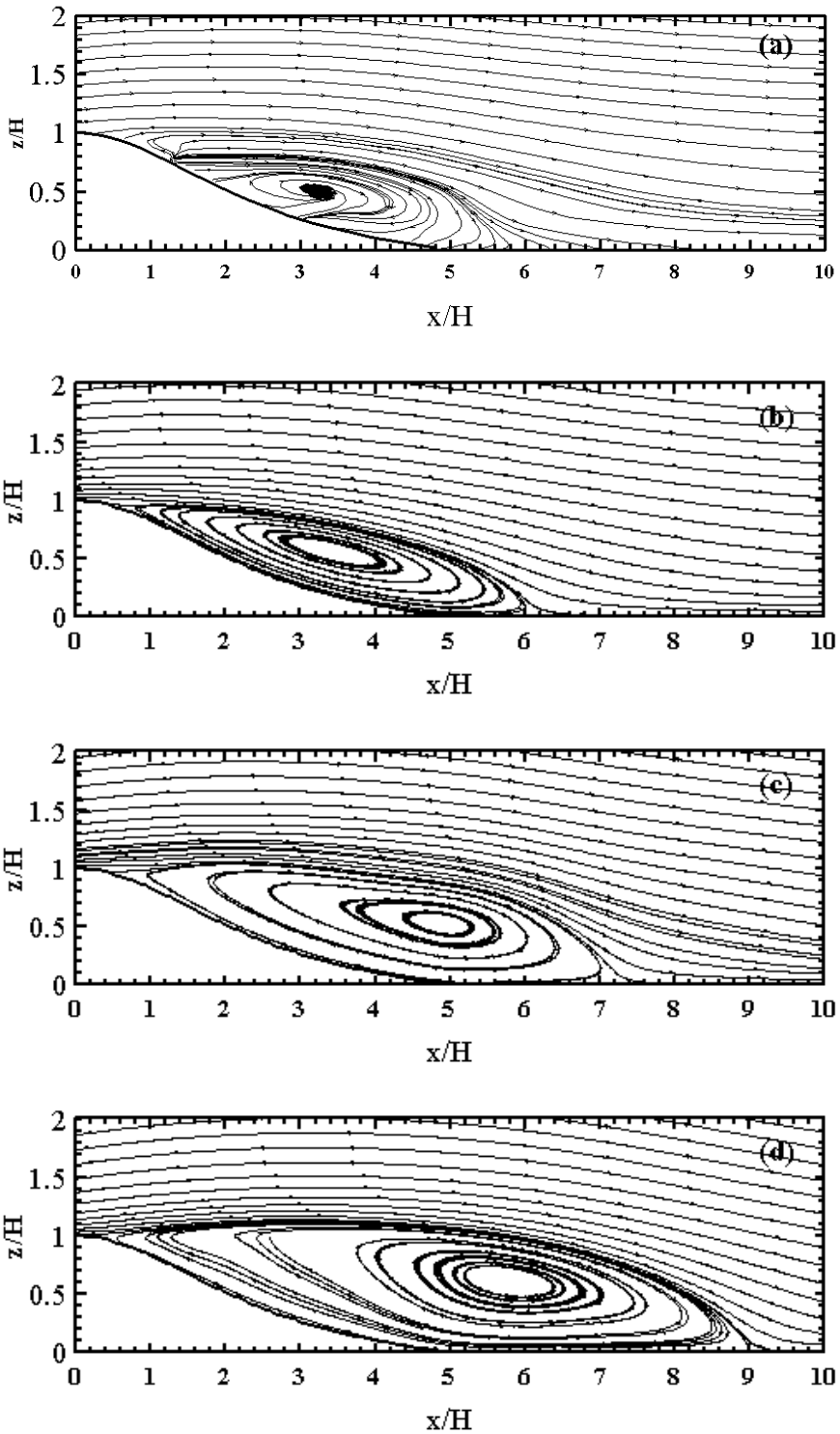

Figure 3: Extension of bubble recirculation region according to (a) Experiments, (b) Cruz and Silva Freire (1998), (c) Mellor (1966) and (d) Nakayama and Koyama (1984).

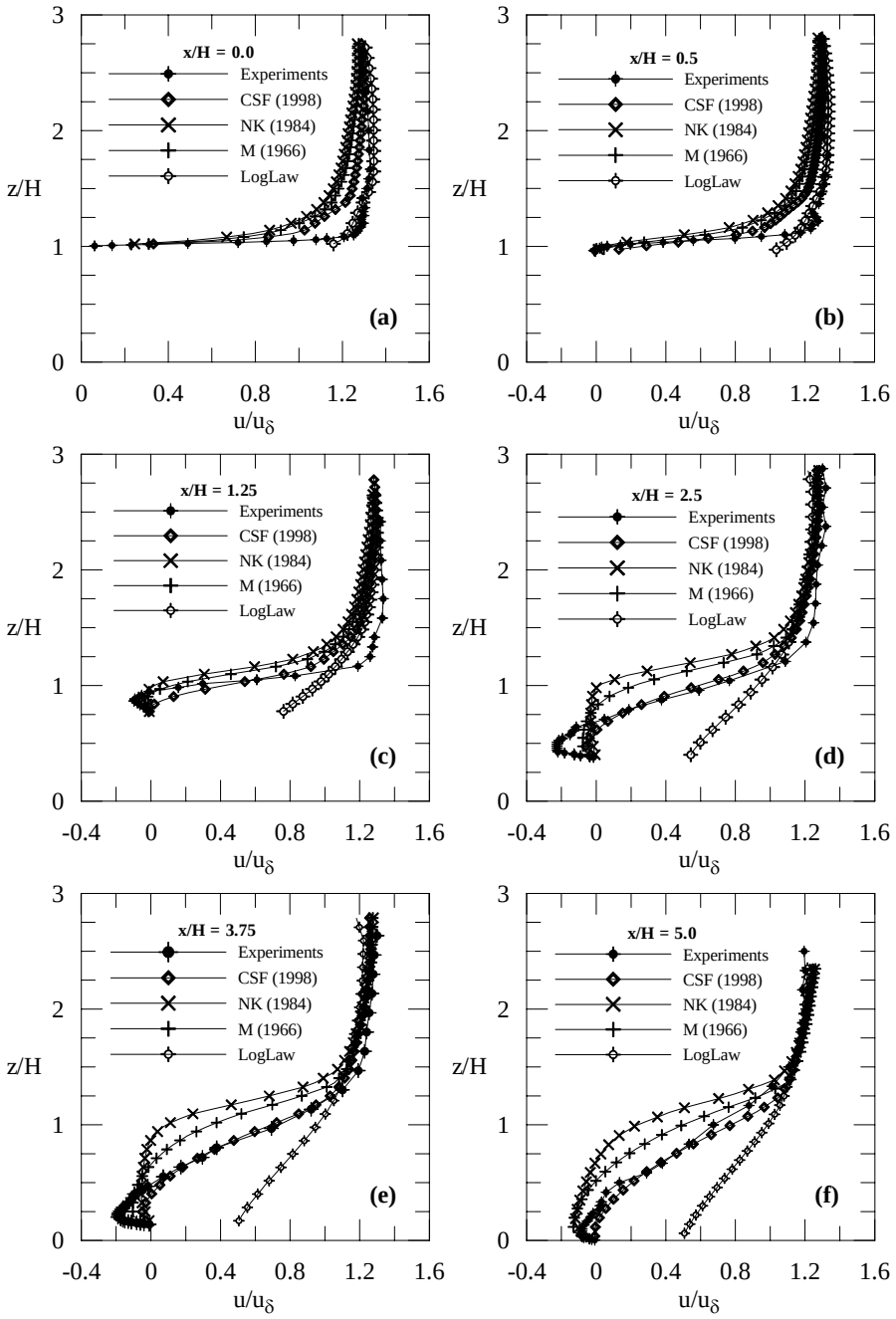

Figure 4: Mean velocity profiles in the region of reverse flow.

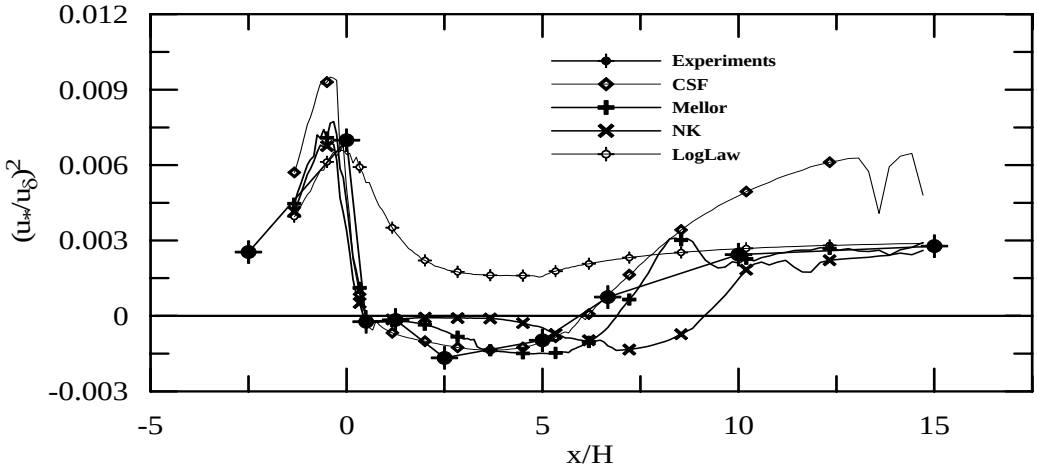

Figure 5: Wall shear stress predictions.

the fundamental difficulty that the number of parameters describing roughness is extraordinarily large owing to the great diversity of geometric forms" (H. Schlichting, Boundary Layer Theory, 7th edition, page 615).

Unfortunately, all surfaces is nature and technology, with a very few exceptions, are rough. That means engineering solutions have to be found to deal with such complex flows. Thus, it is no surprise to find in literature different representations of the same phenomenon – surface roughness – according to the different schools they were developed. Basically two different approaches stand out: the theories advanced by the mechanical engineers and by the meteorologists.

Investigating the flow inside a pipe, and as early as 1923, Hopf identified two types of roughness. If surfaces were formed by relatively coarse and tightly spaced elements (sand grains, cast iron, cement), flow resistance was observed to be proportional to the square of velocity (Reynolds number independence). In this case, the effects of roughness could be expressed with the aid of a single roughness parameter. If, however, surfaces were formed by gentle protrusions distributed over a relatively large area, flow resistance depended both on Reynolds number and on a roughness parameter. A few years later, investigating the flow in a water channel, Einstein and El-Samni (1949) observed that for flow over a rough surface the velocity profiles should be plotted considering that a theoretical wall was set at a distance below the top of the roughness elements. The concept of a displacement in origin was further investigated by Perry and Joubert (1963). These same authors in a sequence paper (Perry et al., 1969) identified two wall geometries that resulted in different log-law behaviors: one type with a reference length based on the size of the roughness (termed a 'k'-type roughness), the other type with a reference length based on the pipe diameter (termed a 'd'-type roughness).

A great difficulty in developing models for flows over rough surfaces is to find reliable measurements for the wall shear stress. For fully developed flows inside a pipe, a simple reading of the pressure drop furnishes the losses. For external flow applications, however, all traditional methods developed for smooth walls including the Preston or Stanton tubes, momentum integral methods and the gradient graphical method are highly inaccurate for application on rough surfaces. As an alternative, more reliable method, Perry et al. (1969) proposed to find the wall shear stress by pressure tapping the roughness elements and assessing their form drag. This can be a good alternative, provided the sizes of roughnesses allow such a practice. Otherwise, the difficulties remain.

The objective of the present work is to assess the current state of turbulent models in regard to the numerical prediction of wall shear stress in turbulent flows over roughness. In particular, we will address a recent and very important controversy. Over the last twenty year, several researchers (see e.g., Wu and Little (1983), Peng and Peterson (1996), Mala and Li (1999), Qu et al. (2000), Guo and Li (2003) and Wu and Cheng (2003)) have claimed that for flows in micro-channels, channels where the internal diameter are less than 250 μm, the classical relations for prediction of pressure losses and of heat transfer do not apply any more. According to these authors, the flows undergo early transition and probable causes of deviation from conventional macroscale results are wall slip effects (gas flow), surface roughness and viscous dissipation. Still, according to Li and Olsen (2006) a common point in early studies is that researchers who found early laminar-turbulent transition concluded that the relative high surface roughness was the major reason for departure from classical results. Our purpose here is to simulate flows in microchannels using the current state of the art for turbulent models so as to obtain a deeper insight onto the applicability or not of the classical expressions. The two test cases will be the flows of Wu and Cheng (2003) and of Li and Olsen (2006). Turbulence models for the numerical simulations will be the eddy-viscosity mixing length (ML), the eddy viscosity shear stress transport (SST) and

the Baseline-ω Reynolds stress model.

4.1. The law of thew wall for flow over roughness

Before considering the experimental data for flows in a microchannel, let us first introduce a short review on the theory of turbulent flow over rough surfaces.

As mentioned before, the description of flows over rough surfaces is greatly complicated by the large number of parameters that are needed to characterize the roughness. This problem was somehow played down in the early experiments by considering homogeneous surfaces, i.e., surfaces where the roughness elements had the same shape and height and were evenly distributed over them. Hopf (1923) showed that if the roughness elements are relatively coarse and tightly spaced, the coefficient of resistance of a pipe is Reynolds number independent. In this case, the characteristics of the rough surface can be expressed in terms of a single length, K_s, the so called relative roughness. If, on the other hand, the protrusions are more sparsely placed and gentle, the resistance coefficient is observed to vary with both the Reynolds number and K_s (Fromm (1923) and Fritsch (1928)).

An extensive experimental program was conducted by Nikuradse (1933) who investigated the flow in sand-roughened pipes. Nikuradse established that, at high Reynolds number, the near wall flow becomes independent of viscosity, being a function of the roughness scale, K_s, the pipe diameter and Reynolds number. He also found that, for the defect layer, the universal laws apply to the bulk of the flow irrespective of the conditions at the wall. The roughness effects are, therefore, restricted to a thin wall layer. For flows in the completely rough regime, that is, flows to which $K_s u_\tau/\nu > 70$ apply, Nikuradse found the following equation to hold

$$\frac{u}{u_\tau} = 2.5 \ln \frac{z}{K_s} + 8.5. \tag{45}$$

Experiments on a hydraulic open channel performed by Einstein and El-Samni (1949) and Moore (1951) showed that a universal expression can be written for the wall region provided the origin for measuring the velocity profile is set some distance below the crest of the roughness elements. This defines a second important characteristic length for the description of roughness. The displacement in origin is normally referred to in literature as the error in origin, ε. A detailed method to determine the displaced origin can be found originally in Perry and Joubert (1963) and more recently in Perry et al. (1986).

Thus, for any kind of rough surface, it is possible to write (Avelino and Silva Freire, 2002):

$$\frac{u}{u_\tau} = \frac{1}{\varkappa} \ln\left[\frac{(z_T + \varepsilon)u_\tau}{\nu}\right] + A - \frac{\Delta u}{u_\tau} \tag{46}$$

where,

$$\frac{\Delta u}{u_\tau} = \frac{1}{\varkappa} \ln\left[\frac{\varepsilon u_\tau}{\nu}\right] + C_i \tag{47}$$

and $\varkappa = 0.4$, $A = 5.0$, and $C_i, i = K, D$; is a parameter characteristic of the roughness (see, for example, Perry and Joubert (1969)).

Equations 46 and 47, although of a universal character, have the inconvenience of needing two unknown parameters for their definition, the skin-friction velocity, u_τ, and the error in origin, ε. A chief concern of many works on the subject is, hence, to characterize these two parameters. These equations are normally summoned for studies on geophysical flows.

If we further consider that Coles's wake hypothesis (Coles (1956)) applies to the outer region of the flow, the law of the wall can be re-written as

$$\frac{u}{u_\tau} = \frac{1}{\varkappa} \ln\left[\frac{(y_T + \varepsilon)u_\tau}{\nu}\right] + A - \frac{\Delta u}{u_\tau} + \frac{\Pi}{\varkappa} W\left(\frac{y}{\delta}\right) \tag{48}$$

where W is a universal function of y/δ and Π is a parameter dependent on the upstream shear stress and pressure distribution.

Equation 48 provides a representation of the velocity field over the whole of the turbulent and defect regions of the boundary layer.

Substitution of (y, u)=(δ, U_∞) into equation 48 furnishes

$$\frac{U_\infty}{u_\tau} = \frac{1}{\varkappa} \ln\left[\frac{\delta + \varepsilon}{\varepsilon}\right] + A - C_i + \frac{2\Pi}{\varkappa} \tag{49}$$

This is a simple algebraic equation that furnishes values of C_f $(= 2u_\tau^2/U_\infty^2)$ for known values of U_∞, δ and ε.

Finally, provided the displacement in origin can be neglected in some applications, the law of the wall can be written as

$$\frac{u}{u_\tau} = \frac{1}{\varkappa} \ln \frac{z}{z_0} \tag{50}$$

where z_0 is the roughness lenght.

Of course, Eqs. 45, 46 and 50 hold between themselves simple algebraic relationships, so that given one characteristic roughness length (say z_0) one can evaluate the others (say, $K_s = e^{8.5\varkappa} z_0 = 29.96 z_0$). However, we must warn the reader to exert some caution here. The relevant characteristic roughness length have been determined in the past based on a large body of works aimed at specific applications. Their straight translation from one type of application to the other may be meaningless. In fact, K_s has been determined for surfaces that are typical in internal flows whereas z_0 has been determined for external flows.

To find a law of resistance for the flow in a pipe, we introduce the coefficient of resistance, λ, through

$$\frac{p_1 - p_2}{L} = -\frac{\partial p}{\partial x} = \frac{\lambda}{D} \frac{\rho}{2} \overline{u}^2, \tag{51}$$

where D denotes the pipe diameter, and $\overline{u}$ is the flow mean velocity.

Then, from Eq. 45 we find

$$\lambda = [2\log(R/K_s) + 1.68]^{-2}. \tag{52}$$

4.2. Turbulence models

Three turbulence models will be used to simulate the flow in a micro-channel: the mixing-length model, the Shear Stress Transport (SST) model and the Reynolds Shear Stress Baseline-ω (RSM-BSL-ω) model. These three models are considered representative enough of the state of the art in turbulence engineering modeling to allow for a good assessment of the numerical computations of the flow over in a channel.

The three chosen models are here considered to be sufficiently well known to dispense a thorough description. Therefore, just a brief description of each model will be offered. For further details the reader is referred to the original sources.

The equations of motion are the Reynolds averaged equations of continuity and momentum for an incompressible flow. Eddy viscosity models consider that the turbulent stresses are related to the mean velocity gradients by a parameter of proportionality, the eddy or turbulent viscosity. Many two-equation turbulence models consider the eddy viscosity to be related to the turbulent kinetic energy, κ, and to the dissipation of turbulent kinetic energy per unit mass, ϵ through $\nu_t = C_\nu \kappa^2/\epsilon$. Transport equations for κ and for ϵ can be derived directly from the Navier-Stokes equations through some algebraic manipulations and some extra subsequent modeling.

Two equation models based on the κ-ϵ formulation are known to suffer limitations in the description of the near wall region since they tend to fail in predicting the correct functional near wall behavior of the logarithmic solution. A perturbation analysis of the κ-ϵ formulation in the near wall region shows that the standard constants yield solutions to the approximate equations that do not follow the classical law of the wall constants, $\varkappa = 0.4$ and $A = 5$. For this reason, a common practice is to use the κ-ϵ model with boundary conditions specified not at the wall, but at some distance above the wall. In this case, the no-slip condition is then replaced by a wall function, the classical law of the wall.

An alternative two equation model that is claimed to circumvent this difficulty is the κ-ω model (Wilcox (1988)). In fact, the great advantage of the κ-ω formulation is supposed to be exactly the near-wall treatment, which can accept higher values of $z^+ = (z u_\tau/\nu)$, the non-dimensional distance from the wall. The κ-ω model has the additional advantage of providing near wall analytical solutions for both the viscous and the fully turbulent regions. In the κ-ω model, the eddy viscosity is taken as $\nu_t = (\kappa/\omega)$.

Despite the superior handling of the wall conditions, the κ-ω formulation struggles with its strong sensitivity to free stream conditions. Thus, given the different zonal strengths and, for that matter, weaknesses of the κ-ϵ and the κ-ω formulations, a good balance can be achieved between both models if a blending is introduced between the κ-ω formulation near the surface and the κ-ϵ model in the outer flow. This solution was proposed by Menter (1994), who introduced the so-called SST-ω model.

A more general way to model a turbulent flow is to compute every component of the Reynolds stress tensor from transport equations derived directly by algebraic manipulations of the Navier-Stokes equations. The resulting loss of information implied by the averaging process must then be recovered by an adequate modeling of each of the terms present in the equations. Most models consider the same basic set of rules to close the equations. All turbulent quantities are considered to be a function of Reynolds stress, κ, ϵ (or alternatively ω), mean flow quantities and related thermodynamics variables. The diffusion of turbulent quantities, in particular,

is taken to be proportional to the local gradient of the quantity. The dissipation of turbulent kinetic energy is supposed to occur at very small scales where turbulence is isotropic. Constants appearing in the models are *ad hoc* so that they must be fixed through experimental calibration. The models also need to be consistent with the common requirements of symmetry, invariance and permutation.

The RSM-BSL-ω model proposes to use a blending function to use the advantages of the two-equation κ-ω model near the wall and a RSM model for the external flow region.

4.3. Flow in micro-channels

We have discussed before that considerations on the laws of resistance for flows in micro-channels have thrown the subject into considerable confusion. Over the last twenty years researchers have found difficult to reach a consensus on whether the classical laws should hold for flows in channels with hydraulic diameters below 200 μm. For example, based on their measurements of pressure losses and of heat transfer, the following authors have suggested the flow to undergo early transition: Wu and Little (1983), Peng and Peterson (1996), Mala and Li (1999), Qu et al. (2000), Guo and Li (2003), Wu and Cheng (2003). Many other researchers, however, have reported that conventional laws can be applied to channel flows: Qu and Mudawar (2002), Judy et al. (2002), Sharp and Adrian (2004), Celata et al. (2004), Li e Olsen (2006).

Here we will use the flow conditions of Wu and Cheng (2003) and of Li and Olsen (2006) to assess the applicability or not of the conventional laws in micro-channels. The simulations were made through the well known code ANSYS CFX, release 5.7. The code solves the Reynolds averaged Navier-Stokes equations (RANS) through a finite-volume approach. The solution strategy consists in solving the momentum equations using a guessed pressure. Next, a pressure correction is obtained which typically needs a large number of iterations to reach a converged solution. The code uses a coupled solver that solves the equations for the flow parameters as a single system. This procedure uses a fully implicit discretization of the equations at any given time. In the present steady state case, the time step behaves like an acceleration parameter to find the approximate solutions in a physically meaningful framework to a time independent solution.

The work of Wu and Cheng (2003) performed an experimental investigation on heat transfer and pressure losses in 13 different trapezoidal silicon micro-channels. Here we analyze the flows in channels number 8 and 10. These channels were chosen for their very different superficial conditions. This is particularly illustrated in Table 5 where the large differences in surfaces roughness are shown. In Table 5, K denotes the rms value of the surface roughness and D_h the hydraulic diameter of the pipe.

Table 5: Geometric parameters of channels (Wu and Cheng, 2003). Dimensions are given in μm.

Channel	W_t (top)	W_b (bottom)	H (height)	K/D_h
8	171.70	0	110.8	$3.62\ 10^{-5}$
10	168.70	0	108.9	$1.09\ 10^{-2}$

The conditions for the experiments of Wu and Cheng (2003) were such that the flow was laminar. Under this condition classical theory says that surface roughness does not affect the laws of resistance. Wu and Cheng (2003), however, have implied in their work that as pipe diameter decreases, surface roughness should becomes important. Thus, present solution strategy consisted in simulating the flow with the RSM-BSL-ω model, incorporating the wall roughness effects through the formulation of Nikuradse.

The major problem then was to evaluate K_s from a given value of K. To do that we followed the main practice of considering $z_0 = 0.1\ K$. Then using the transformation $K_s = z_0 \exp(8.5\varkappa)$, the effective roughness was estimated. The findings are shown in Table 6.

Table 6: Values of K_s for the data of Wu and Cheng (2003). Dimensions are given in μm.

Channel	K	K_s
8	0.003	0.9
10	0.009	2.728

The resistance coefficient, λ, was evaluated from the numerical data through Eq. 51. The pressure values p_2 and p_1 were taken directly from the computations and D was considered to be the hydraulic diameter. The numerical values are compared with the experimental values of Wu and Cheng and the Blasius (1911), Collebrook (1939) and White (1991) resistance formulas in Fig. 6.

The formula of Blasius is empirical and holds for smooth surfaces; it can be written as

$$\lambda = 0.3164 R^{-0.25}. \tag{53}$$

The experimental correlation of Colebrook (1939) is supposed to cover the whole transition region from hydrodynamic smooth to fully rough surface; it can be cast as

$$\frac{1}{\sqrt{\lambda}} = 1.74 - 2\log\left(\frac{K_s}{R} + \frac{18.7}{R\sqrt{\lambda}}\right). \tag{54}$$

For two dimensional, laminar flow between parallel walls, White (1991) proposed to consider

$$\lambda R(L^+) = \frac{3.44}{(L^+)^{0.5}} + \frac{24 + \frac{0.674}{4L^+} - \frac{3.44}{(L^+)^{0.5}}}{1 + \frac{2.9\,10^{-5}}{(L^+)^2}}, \tag{55}$$

where

$$L^+ = \frac{L}{D_h}\frac{1}{R}. \tag{56}$$

accounts for wall entrance effects.

Clearly, the numerical results agree quite well with the predictions given by Blasius' equation. In fact, we must notice that the equation of Blasius was derived for flow in a circular pipe. Our problem geometry consists of a trapezoidal channel, which should yield higher values of λ. Therefore, the present results are consistent and indicate that very much probably the experimental data have some serious problems. There no reason why such a large discrepancy should occur between the predictions of Blasius and the experimental data. For such a low Reynolds number all classical laws should hold. And, indeed, this is exactly what the present analysis points to.

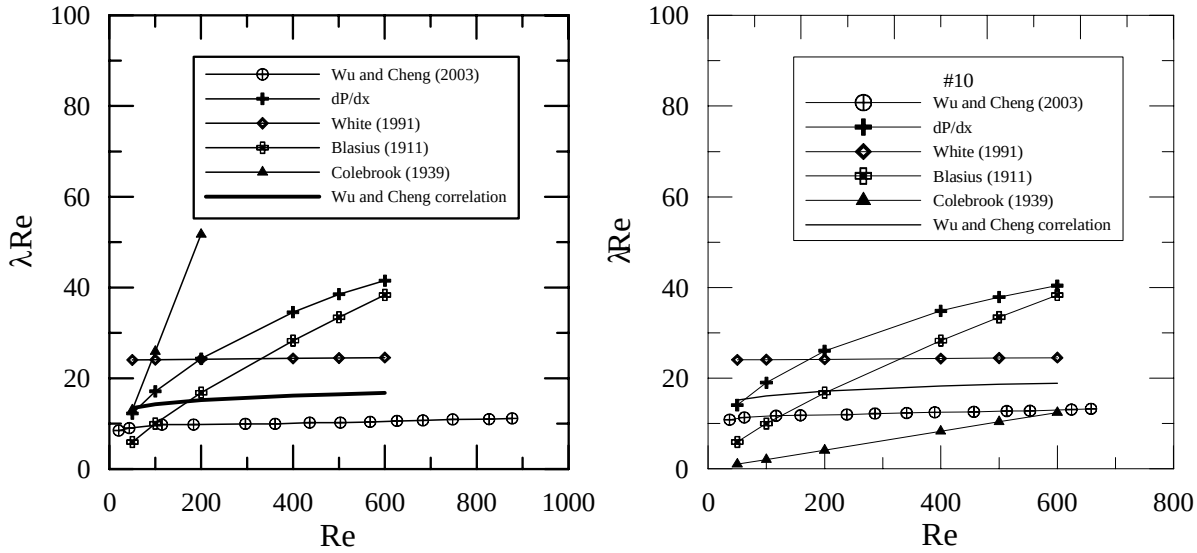

Figure 6: Predictions of coefficient of resistance according to the data of Wu and Cheng (2003).

Li and Olsen (2006) used microscopic particle image velocimetry (microPIV) to investigate rectangular micro-channels with hydraulic diameters ranging from 200 to 640 μm and Reynolds number ranging from 200 to 3971. These authors did not identify early transition and made full measurements of local mean and fluctuating velocity profiles.

To simulate their flow conditions, we use the same procedure as before for the flow of Wu and Cheng (2003). Thus for a value of $K = 0.008$ μm, we find $K_s = 0.02424$ μm. The simulations made use of all three turbulence models suggested previously: ML, SST and RSM-BSL-ω. The typical details are shown in Table 7. The results were obtained with the following computer architecture: Intel D875PBZ Motherboard (With on-board Gigabit Ethernet network interface), Pentium 4, 3.0Gz, 1Mb Cache, 2 Gb DDR400 in dual mode (2 x 512 Mb), 200 GB SATA HD.

The general flow pattern in the rectangular channel is shown in Fig. 7. The eight recirculating cells that are formed can be easily observed. The mean and fluctuating longitudinal velocity profiles are shown in Fig. . The overall agreement of all models is very good. Please note that Li and Olsen's measurements do not span the

Table 7: Simulation Details (Li and Olsen, 2006).

Model	Mesh Elements (Hexahedron)	Inlet speed (m/s)	Total run time
Mixing-length	1,233,400	7.3684	45:40
SST	1,233,400	7.3684	3:09:32
RSM-BSL-ω	1,233,400	7.3684	5:23:02

near wall region so that drawing much conclusion on flow behavior there is difficult. The SST and RSM-BSL models, being based on the ω-equation present the same near wall results. These are quite distinct from the ML results.

The longitudinal velocity fluctuations predictions are not good. The numerical computations much underestimate the values of $\sqrt{\overline{u'^2}}$, in particular, in the near wall region. The roughness effects, however, are well illustrated. Inclusion of K_s in the simulations much improves the results.

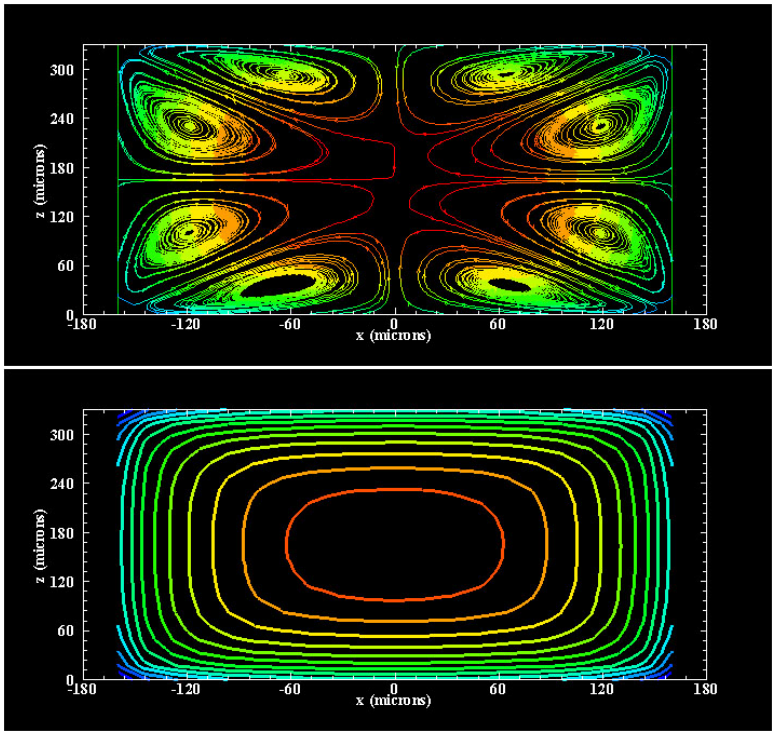

Figure 7: Streamline and isoline profiles according to the data of Li and Olsen (2006).

Finally, Fig. 9 shows a parametric study regarding the velocity prediction dependence on K_s. The three very close values of $K_S = 0.02424$, 0.02121 and 0.01818 give acceptable results. The other two extreme values, $K_s = 0.0$ and 0.07272, provide predictions that are clearly off the mark. We have, therefore, plain evidence that roughness effects are important in micro-channel flow predictions and that the current state of knowledge is capable of providing very good estimates of flow properties in channels.

5. Conclusion

We have shown how some difficult problems in engineering can be given a good representation provided their fundamental knowledge is developed from asymptotic arguments combined with rigorous *ad hoc* experimental evidence. The problem of a separating flow shows how some simple modelling based on algebraic turbulence models can be combined with scaling arguments and local analysis to provide analytical near wall solutions that can be used as boundary conditions for numerical simulations of flows over steep hills. We have, in particular, shown that the region of reverse flow can be well described by those solutions.

The flow over rough surfaces in micro-channels was also numerically simulated to show how the current state of the art in flow modelling is capable of furnishing results that are consistent with the classical laws and the experimental data. Thus, the present results suggest that measurements that report early transition must be seen with much caution. There exists a strong possibility that these experiments be contaminated by uncertain

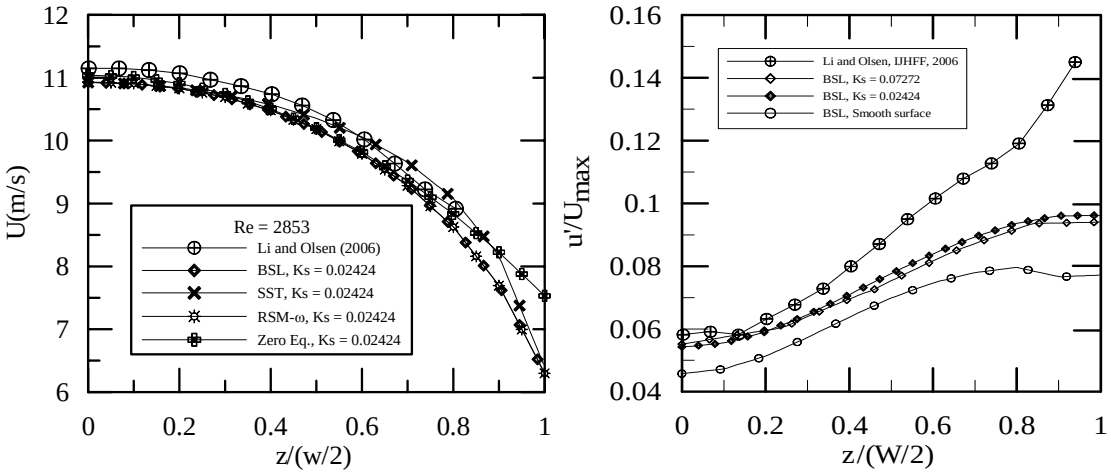

Figure 8: Mean and fluctuating longitudinal velocity profiles according to the data of Li and Olsen (2006).

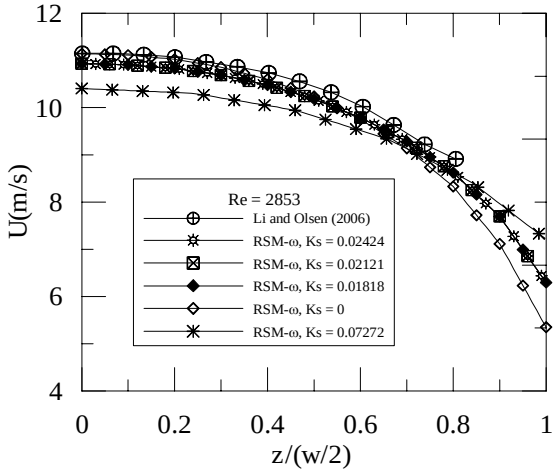

Figure 9: Parametric study on the dependence of velocity predictions on values of K_s (data of Li and Olsen (2006)).

readings and poor planning and execution.

The challenges ahead of any researcher willing to work with flow separation or flow over rough surfaces are many. The mathematical description of the flow near to a separation point is still a very difficult and open problem. Much further studies are necessary before a complete picture of the problem is drawn. The recent advances in computational fluid dynamics have made available to researchers a host of new results that will be of great help in identifying relevant scales to the problem and the local solution behaviour. The expectation then is that much more appropriate turbulence models can be developed.

Finally, we must point out to the reader that a problem where very little progress has been achieved over the last years is separated flow over rough surfaces. The present text has been written with the purpose of providing part of the basic material that should allow such a leap forward. Details on how this can be made will be given in another communication.

Acknowledgments. APSF is grateful to the Brazilian National Research Council (CNPq) for the award of a Research Fellowship (Grant No 304919/2003-9). The work was financially supported by CNPq through Grant No 472215/2003-5 and by the Rio de Janeiro Research Foundation (FAPERJ) through Grants E-26/171.198/2003 (Pronex Research Project) and E-26/152.368/2002.

6. References

Avelino, M.R. and Silva Freire, A.P. 2002 IJHMT **45** 3143-3153

Batchelor, G. 1967 *An Introduction to Fluid Dynamics* CUP

Brison, J.F., Buffat, M., Jeandel, D. and Serres, E. 1985 *Numerical Methods in Laminar and Turbulent Flows* Pineridge Press

Brun, G. 1988 *Thèse de Doctorat* École Centrale de Lyon

Bush, W.B. and Fendell, F.E. 1972 JFM **56** 657-681

Celata, G.P., Cumo, M. and Zummo, G. 2004 ETFS **28** 87-95

Cruz D.O.A. and Silva Freire A.P. 1998 IJHMT **41** 2097–2111

Cruz D.O.A. and Silva Freire A.P. 2002 IJHMT **45** 1459–1465

Coles, D. 1956 JFM **1** 191-226.

Einstein, H.A. and El-Samni, E.-S.A. 1949 Review of Modern Physics **21** 520–524.

Fontoura Rodrigues, J.L.A. 1990 *Thèse de Doctorat* École Centrale de Lyon

Fromm, K. 1923 ZAMM **3** 339-358

Fritsch, W. 1928 ZAMM **8** 199-216

Goldstein, S. 1938 *Modern Developments in Fluid Dynamics I, II* Clarendon Press

Goldstein, S. 1948 QJMAM **1** 43-69

Guo, Z.Y and Li, Z.X. 2003 IJHFF **24** 284-298

Hopf, L. 1923 ZAMM **3** 329-339

Hughes, T.J.R. and Brooks, A. 1979 *Element Methods for Convection Dominated Flows* ASME-AMD **34**

Judy, J., Maynes, D. and Webb, B. W. 2002 IJHMT **45** 3477-3489

Kaplun, S. 1967 *Fluid Mechanics and Singular Perturbation* Academic Press N.Y.

Kelly, D.W., Nakazawa, S. and Zienkiewcz, S. 1980 *Int. J. Num. Meth. Engng.* **3** 269–289.

Landau, L.D. and Lifschitz, E.M. 1959 *Fluid Mechanics* Pergamon Press

Launder, B.E. and Spalding, D.B. 1974 *Computer Methods in Applied Mechanics* **3** 269–289

Li, H. and Olsen, M.G. 2006 IJHFF **27** 123-134

Loureiro, J.B.R., Soares, D.V., Fontoura Rodrigues, J.L.A., Pinho, F.T. and Silva Freire, A.P. 2006 BLM in press

Mala, G.M. and Li, D. 1999 IJHFF **20** 142-148

Mellor, G.L. 1966 JFM **24** 255–274

Mellor, G.L. 1972 IJES **10** 851–873

Melnik, R.E. 1989 Computers and Fluids **17** 165–184

Millikan, C.B. 1939 *Proc. 5th Int. Congress on Applied Mechanics* J. Wiley N.Y.

Moore, W.L. 1951 Ph. D. Thesis State University of Iowa

Nakayama, A. and Koyama, H. 1984 AIAA Journal **22**, 1386–1389

Nikuradse, J. 1933 Stromungsgesetze in Rauhen Rohren, V. D. I. Forshungsheft No 361 1933

Peng, X.F. and Peterson, G.P. 1996 IJHMT **12** 2599-2608

Perry, A.E. and Joubert, P.N. 1963 JFM **17** 193-211.

Perry, A.E., Schofield, W.H. and Joubert, P.N. 1969 JFM **37** 383-413.

Perry, A.E., Lim K.L. and Henbest, S.M. 1987 JFM 1987 **177** 437–466.

Prandtl, L. 1925 ZAMM **5**, 136–139

Qu, W.L., Mala, G.M. and Li, D.Q. 2000 IJHMT **43** 353-364

Qu, W. and Mudawar, I. 2002 IJHMT **45** 2549-2565

Schlichting, H. 1979 *Boundary Layer Theory* McGraw Hill

Sharp, K.V. and Adrian, R.J. 2004 Exp. Fluids **36** 741-747

Stewartson, K. 1969 Mathematika **16** 106-121

Simpson, R.L., Chew, Y.T. and Schivaprasad, B.G. 1981 JFM **113** 23–51

Stratford, B. S. 1959 JFM **5** 1–16

Sychev, V.V. and Sychev, V.V. 1980 USSR Comput Maths Math Phys **20** 133–145

Tennekes, H. and Lumley, J.L. 1972 *A First Course on Turbulence* MIT Press

Yajnik, K.S. 1970 JFM **42** 411–427

White, F. M. 1991 *Viscous Fluid Flow* McGrawHill NY

Wu, H.Y. and Cheng, P. 2003 IJHMT **46** 2547-2556

Wu, P.Y. and Little, W.A. 1983 Cryogenics **23** 273-277